

Micromere lineages in the glossiphoniid leech *Helobdella*

Françoise Z. Huang¹, Dongmin Kang^{1,*}, Felipe-Andres Ramirez-Weber^{1,†}, Shirley T. Bissen² and David A. Weisblat^{1,‡}

¹Department of Molecular and Cell Biology, 385 LSA, University of California, Berkeley, CA 94720-3200, USA

²Department of Biology, University of Missouri, St Louis, MO 63121-4499, USA

*Present address: Department of Biology, Stanford University, Stanford, CA 94305-5020, USA

†Present address: Department of Biochemistry and Biophysics, University of California, San Francisco, CA 94143, USA

‡Author for correspondence (e-mail: weisblat@uclink4.berkeley.edu)

Accepted 31 October 2001

SUMMARY

In leech embryos, segmental mesoderm and ectoderm arise from teloblasts by lineages that are already relatively well characterized. Here, we present data concerning the early divisions and the definitive fate maps of the micromeres, a group of 25 small cells that arise during the modified spiral cleavage in leech (*Helobdella robusta*) and contribute to most of the nonsegmental tissues of the adult. Three noteworthy results of this work are as follows. (1) The c''' and dm' clones (3d and 3c in traditional nomenclature) give rise to a hitherto undescribed network of fibers that run from one end of the embryo to the other. (2) The clones of micromeres b'' and b''' (2b and 3b in traditional nomenclature) die in normal development; the b'' clone can be rescued to assume the normal c'' fate if micromere c'' or

its clone are ablated in early development. (3) Two qualitative differences in micromere fates are seen between *H. robusta* (Sacramento) and another *Helobdella* sp. (Galt). First, in *Helobdella* sp. (Galt), the clone of micromere b'' does not normally die, and contributes a subset of the cells arising exclusively from c'' in *H. robusta* (Sacramento). Second, in *Helobdella* sp. (Galt), micromere c''' makes no definitive contribution, whereas micromere dm' gives rise to cells equivalent to those arising from c''' and dm' in *H. robusta* (Sacramento).

Key words: Cell cycle, Cell lineage, Equivalence group, *Helobdella*, Leech, Lophotrochozoa, Spiralia

INTRODUCTION

Spiral cleavage is characterized by cell divisions that are oriented obliquely with respect to the animal-vegetal (A-V) axis of the embryo. This results in an offset of approximately 45° between animal and vegetal tiers of sister cells. The offset of successive tiers of cells alternates between clockwise and counterclockwise due to corresponding alternations in the spindle orientations with each round of divisions. The divisions are typically unequal, beginning with third cleavage and generating quartets of animal micromeres and vegetal macromeres.

Roughly ten protostome phyla are classified as exhibiting spiral cleavage (Brusca and Brusca, 1990). Of these, all but the arthropods fall within the Lophotrochozoan clade, as defined by recent molecular phylogenies (Aguinaldo et al., 1997), and the question of whether the division patterns seen in basal arthropods represent true spiral cleavage or convergence was debated even prior to this time (Anderson, 1973). By contrast, it seems beyond question that the spiral cleavage patterns (and trochophore larvae) seen in mollusks and annelids are homologous. Thus, comparisons of cell fates and cell fate specification processes between annelids and mollusks may yield insights about the nature of the ancestral Lophotrochozoan, and into how modern animals with

such different body plans could have evolved from that ancestor.

The modified pattern of spiral cleavage in glossiphoniid leech embryos generates three size classes of blastomeres, called teloblasts, macromeres, and micromeres (Fig. 1) (Bissen and Weisblat, 1989; Sandig and Dohle, 1988). In the traditional nomenclature for spiralian embryos, micromeres and macromeres were defined according to the relative positions of sister cells along the A-V axis. This system has led to ambiguities as to the names of clearly homologous cells in different species (e.g. Fischer, 1999; Sandig and Dohle, 1988). For simplicity, we therefore define micromeres as the 25 small cells arising during cleavage (Bissen and Weisblat, 1989; Smith and Weisblat, 1994), independent of the orientation of the division by which they arise.

The micromeres give rise to a mixture of definitive and provisional progeny, in nonsegmental neural and non-neural tissues (Nardelli-Haeffiger and Shankland, 1992; Smith and Weisblat, 1994; Weisblat et al., 1984). Micromere derivatives are also important in determining cell fates of certain segmental founder cells (Ho and Weisblat, 1987; Huang and Weisblat, 1996). Moreover, certain micromeres in leech embryos are homologous with blastomeres that have different fates in the embryos of other annelids and mollusks (Damen and Dictus, 1994; Dohle, 1999). Another question of interest

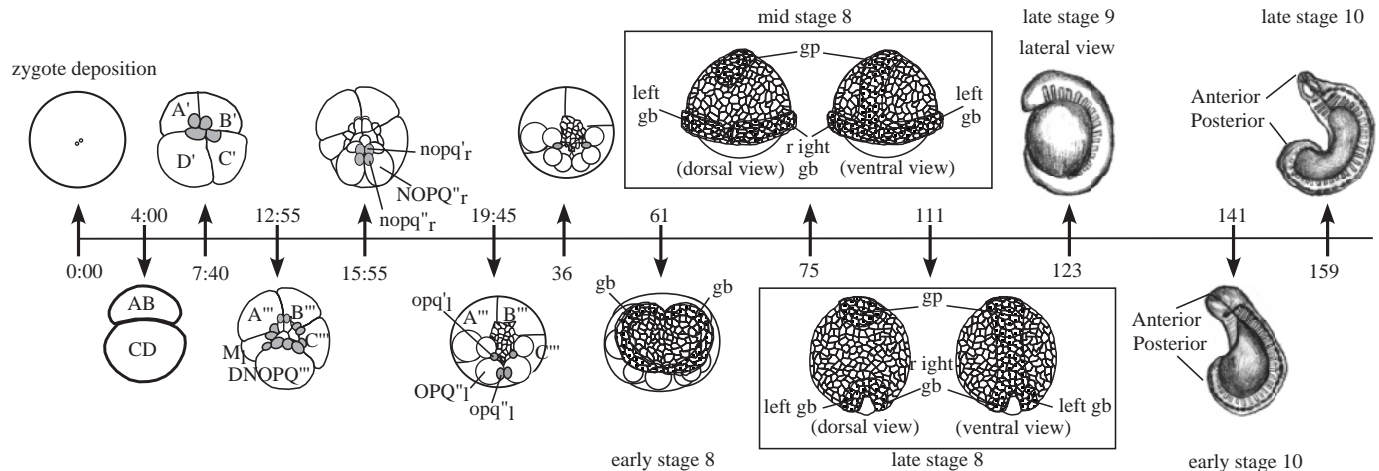


Fig. 1. Time line showing relevant stages of *Helobdella* development. The numbers on the time line are given in hours after zygote deposition (hours AZD). Micromeres arise by stereotyped cleavages; shaded cells at 7:40, 12:55, 15:55, 19:45 and at 36 hours AZD represent the micromeres born since the previous time point (for details, see Fig. 2). According to the numerical staging system of Fernández (Fernández, 1980), the micromeres are born during stages 4a to 6b, but the strictly temporal staging system is required for most of the experiments described here. For some fate-mapping experiments, embryos in later stages are designated less precisely using the numerical staging system.

is how cell fates are assigned so that micromeres derived from spiral cleavages contribute to the bilaterally symmetric body plan of the leech. To understand how cell fates are assigned in the micromere lineages in leech and how cell fate decisions might have evolved within the spiralia, we have analyzed the micromeres in embryos of the leech *Helobdella robusta* with respect to cell cycle composition, timing and orientation of their initial divisions, and the distribution of their clones in the juvenile. For these purposes, we have fate mapped micromeres using fluorescent lineage tracers injected at the time of their birth (stages 4a-6b) to identify their progeny in the late embryo (stage 10), and we have used video time-lapse microscopy and S-phase labeling [5-bromo-2'-deoxyuridine 5'-triphosphate (BrdUTP) incorporation] to analyze cell cycle composition and mitotic patterns. With certain exceptions, these experiments reveal stereotyped cell division patterns, the fates and clonal distribution patterns for the individual micromeres. The results allow us to identify a new equivalence group, lay a groundwork for understanding the morphogenesis of the proboscis and other nonsegmented tissues, including some hitherto undescribed neurons, and to compare leeches and gastropod mollusks (another derived spiralian group) in terms of the symmetry relationships of their micromere clones. Finally, we have inadvertently discovered clear and reproducible differences in micromere fates of four micromeres between embryos from two nearby populations of what we had assumed was the same species, *H. robusta*. This result provides a measure of the extent to which developmental mechanisms can vary while conserving a particular endpoint.

MATERIALS AND METHODS

Embryos

Unless specified, the experiments reported here employed embryos of *H. robusta* (Shankland et al., 1992). They were obtained from animals collected from a minor tributary of the American River in Sacramento, California or, more commonly, from a laboratory breeding colony

founded with such animals. Embryos for some experiments were obtained from leeches collected near Galt, California. Where necessary, to distinguish between the two, they are designated as *H. robusta* (Sacramento), and *Helobdella* sp. (Galt), respectively.

Helobdella eggs are fertilized internally and arrest at metaphase I until zygote deposition (Fernandez and Olea, 1982; Wedeen et al., 1990). Individual clutches of embryos, typically deposited over the course of an hour or more, were divided into subpopulations of more closely synchronized siblings by pooling embryos that underwent a selected cell division within a time window of 5-10 minutes. For example, to analyze the cell cycle and mitotic patterns of micromere d', large clutches of embryos were divided into smaller, more synchronous groups as blastomere CD cleaved to yield blastomeres C and D, which is the parent cell of micromere d'. Micromeres are designated according to Bissen and Weisblat (Bissen and Weisblat, 1989) (Fig. 1). For the purpose of comparing one micromere lineage to another, it is useful to indicate the timing of cell divisions in terms of clonal age at which they occur, i.e. hours since the birth of the given micromere. To place events within the context of overall development, we also designate timings in terms of hours after zygote deposition (AZD).

Lineage tracing

Micromeres were pressure-injected (Smith and Weisblat, 1994) about 20 minutes after their birth with either 1.1'-dioctadecyl-3,3,3',3'-tetramethylindocarbocyanine perchlorate (diI; Molecular Probes, Eugene, Oregon, USA; 50 mg/ml in ethanol, then diluted 1/50 in walnut oil) or with a mixture of lysinated, rhodamine-, or fluorescein-conjugated dextran (RDA or FDA, Molecular Probes; 75 mg/ml final concentration) and fast green (1% final concentration) in 0.2 M KCl. Injected embryos were cultured in *Helobdella* embryo (HL) medium (4.8 mM NaCl, 1.2 mM KCl, 2 mM MgCl₂, 8.0 mM CaCl₂ and 1 mM maleic acid, pH 6.6) at 23°C. For regular fluorescence microscopy, embryos were counterstained with Hoechst 33258 (1 µg/ml final concentration) after fixation. For confocal microscopy, embryos were fixed in 4% formaldehyde, 0.75× PBS, overnight at 4°C, then rinsed in 1× PBS, incubated for 1 hour in a solution of 50 µg/ml of RNase in 1× PBS at 37°C, rinsed in sodium chloride, sodium citrate buffer (1× SSC) (Sambrook et al., 1989), incubated in 16.7 µM Sytox Green (Molecular Probes, Eugene, OR) in 1× SSC for 45 minutes, rinsed in 1× SSC and transferred to 100% glycerol for viewing.

Cell ablations

In some experiments, specific micromeres were killed prior to their first division by 'over-injection', i.e. injecting the cell with RDA or FDA until the cell was seen to lyse, as judged by the abrupt leakage of the fast green tracking dye. In other experiments, clones of specific micromeres were killed by photoablation. For this purpose, the parent micromere was injected with FDA as described above, allowed to develop normally for various lengths of time and then exposed to UV light for 2-4 minutes 4× planapo objective on a fluorescence microscope (Nikon E800 equipped with a 100 W Hg bulb) through the fluorescein filter set. This treatment did not bleach the FDA completely from the labeled clone, but did kill the cells; 24 hours later, cells in the FDA-labeled clone had failed to divide and either remained rounded up or had lysed, as judged by the appearance of widely distributed fluorescent debris. This treatment did not affect the development of RDA-labeled clones.

Nomenclature for micromere progeny

To designate progeny within the micromere lineages, we named the cells arising at each division according to the parent cell and their relative positions along the main axis of the division by which they arise, as is used for the nematode *Caenorhabditis elegans*. Trying to map the definitive axes (anterior/posterior, dorsal/ventral and left/right) onto the early embryo is difficult because of the cell movements involved in later development. To avoid this problem, we designated the relative positions of sister cells with respect to the polar coordinates as follows: for cell divisions that occur mainly parallel to the surface, sister cells were designated either animal/vegetal or left/right, as viewed from the nearest surface of the embryo; and for divisions that occur mainly parallel to the radius of the embryos, sister cells were designated as deep/superficial. For oblique divisions, we have named cells with respect to the primary axis of the division.

Video microscopy

Micromeres labeled with diI are more resistant to damage by the exciting fluorescence illumination than those labeled with RDA. Moreover, the contours of diI-labeled cells are more easily resolved because the fluorescence is concentrated in the cell membranes rather than in the cytoplasm. Therefore, diI labeling was used to visualize cell divisions in living embryos. For this purpose, embryos were mounted 1 hour after diI injection, animal side up, in precast wells formed in a thin slab of 0.75% agarose in HL medium (Symes and Weisblat, 1992). The agarose slab was then mounted between a glass slide and coverslip, the edges of which were then sealed with parafilm to prevent dehydration. The mounted embryos were then observed by brightfield and fluorescence microscopy (Zeiss Axiophot). Images of developing cells were taken every hour for 12-36 hours with an MTI 3CCD camera and digitized on a Macintosh computer via NIH image software. Between taking images, the preparation was stored at 23°C. The injected walnut oil remains as a droplet within the injected cell or one of its progeny even after the diI has diffused into the cell membranes. Because this droplet could affect estimates of cell size, RDA labeling was used in assessing whether a given cell division was equal or unequal. For this purpose, we define unequal cell divisions as those in which the size difference between sister cells was immediately obvious, which correlates with diameter ratios of ~2 or more between the sister cells; otherwise, the cell divisions were described as equal.

Other images were obtained using either a CCD camera (Roper Scientific, Trenton, NJ) mounted on a upright fluorescence microscope (Nikon E800) controlled by a PC computer with commercial image acquisition and processing software (Metamorph, UIC, Downingtown, PA), or using a confocal microscope (Biorad MRC 1024).

BrdUTP incorporation and immunocytochemistry

BrdUTP incorporation was used to label S-phase nuclei. Clutches of

at least 40 embryos were isolated from the adult and subdivided into developmentally synchronized subgroups (three to seven embryos each), after which specific micromeres were injected with RDA as described above. At various time intervals, embryos in selected subgroups were injected with a mixture containing 50 mM BrdUTP (Sigma), 1% fast green and 0.05 N KCl. For this purpose, the injection was made into any blastomere in the embryo, because the BrdUTP diffuses readily from cell to cell in these early stages (Bissen and Weisblat, 1989). Injected embryos were incubated for 15 minutes, then fixed in 4% formaldehyde in 100 mM cacodylic acid (pH 7.3) for 1 hour, rinsed twice in 1× PBS, then manually devitellinized in 1× PBS. Devitellinized embryos were treated with 2 N HCl in 1× PBS for 1 hour, after which the acid was neutralized by two rinses of 3 minutes each with 0.1M sodium borate, pH 8.5. Embryos were subsequently incubated for 1-3 hours in extraction solution [1× PBS; 10% normal goat serum (NGS), Sigma, St Louis, MO; 1% Triton X-100]. Extraction solution was replaced by a solution of primary anti-BrdU antibody (Boehringer Mannheim, Indianapolis, IN, mouse monoclonal anti-BrdU antibody stock diluted 50-fold in extraction solution) for 12-24 hours. Embryos were rinsed for 1 hour with extraction solution, then incubated in secondary antibody [1:500 HRP-conjugated goat anti mouse (Roche, Indianapolis, IN) in extraction solution] for 12-24 hours, rinsed again in extraction solution (45 minutes-12 hours). Embryos were then rinsed briefly in 1× PBS, then transferred to a solution of 0.5 mg/ml 3,3'-diaminobenzidine (DAB, Sigma) in 1× PBS for 15 minutes before adding H₂O₂ to a final concentration of 0.03%. The color reaction was monitored under a dissecting scope and allowed to proceed until the first sign of rising background, at which time the embryos were rinsed in 1× PBS and transferred in 80% glycerol in 0.1 Tris, pH 8.8. All rinses and incubations were at room temperature.

RESULTS

Micromere lineages

To study micromere lineages, we used two complementary techniques. Video time-lapse microscopy of micromeres labeled with fluorescent lineage tracers allows us to determine cell cycle duration, defined as the interval between two cytokineses. However, this technique is limited by the need to expose the embryos to UV light. To be sure that the embryos were developing normally, we took fluorescence images no more than once per hour. This resulted in ambiguities in tracking cell divisions, especially once the clone of interest had increased to more than three cells. To overcome this problem, we identified progeny of recent divisions as they entered S phase of the next cell cycle, using immunohistochemical detection of BrdUTP incorporation in carefully staged embryos in which one or more micromere clones were marked by previously injected lineage tracer (see Materials and Methods). The deduced micromeres lineages are shown in Fig. 2. Although BrdUTP incorporation was analyzed mainly to identify mitotic sister cells, these experiments also allowed us to determine the duration of S phase and thus the composition of cell cycle in some micromeres and their progeny (Table 1).

Primary quartet micromeres (a'-d')

The primary quartet of micromeres arise sequentially in three steps during third cleavage: first d', then c', then a' and b' together (Bissen and Weisblat, 1989; Sandig and Dohle, 1988). We confirm that glossiphoniid leeches deviate from the standard spiralian pattern in that at each round of division the B quadrant micromeres arise with opposite handedness to those

Table 1. Summary of micromere cell cycle and cell fate data for *H. robusta*

Cell	Total*	M+G1 [†]	S [‡]	G2 [§]	N [¶]	Size**	Contribution at st 10 (160 h AZD)
d'	8.75	(0.5)+(-0)	≤0.25	-	-	-	Neurons to supraesophageal ganglion, putative longitudinal muscles and other cells to proboscis, epithelial cells to proboscis, proboscis sheath, prostomium and provisional integument (Figure 4F).
d'.a	2.75	(0.5)+(-0)	≤0.25	2.5	-	-	Clones of a' and d' are situated across the embryonic midline from those of b' and c', respectively (Weisblat et al., 1984; Nardelli-Haefflinger and Shankland, 1993).
d'.v	-	(0.5)+(-0)	1	>7	-	-	
d'.aa	3±0.5	(0.5)+(-0)	0.25	3	-	-	
d'.av	-	(0.5)+(-0)	1	>5	-	-	
d'.aaa	-	(0.5)+(-0)	.5	-	-	-	
d'.aav	-	(0.5)+(-0)	>1.5	-	-	-	
b'	9.0	(0.5)+(-0)	≤0.25	-	-	-	Cell cycle composition for micromeres c' and a' is the same as for d' and b', respectively, and is omitted.
b'.a	2.75	(0.5)+(-0)	≤0.25	2.5	-	-	
b'.v	-	(0.5)+(-0)	1.75	-	-	-	
b'.aa	3.2	(0.5)+(-0)	≤0.25	2.9	-	-	
b'.av	-	(0.5)+(-0)	1.75	-	-	-	
b'.aaa	-	(0.5)+(-0)	≤0.25	-	-	-	
b'.aav	-	(0.5)+(-0)	>0.5	-	-	-	
a''	24±1	(0.5)+(-0.12)	0.83±0.12	23±0.12	32	=	Bilaterally symmetric sets of cells to proboscis, roughly midway along its length (Figure 4, C, E); by stage 11, these cells project narrow processes, suggesting that they are differentiating as neurons and/or connective tissue (Figure 4D).
a''.d/s	-	(0.5)+(-0)	1.75	-	-	-	
c''	24±1	(0.5)+(-0.12)	0.75±0.12	23±0.5	112	=	
c''.d/s	5	(0.5)+(-0)	≤0.25	4	-	-	
b''	25±2	(0.5)+(-0.12)	≥0.5	23±2	122	=	No contribution. Can replace c'' if the latter is absent. (Figure 7 and 8).
b''.d/s	-	(0.5)+(-0)	±0.5	>5	-	-	
a'''	24±1	(0.5)+(-0)	0.75±.25	22±1	142	=	Putative neurons and connective tissue to supraesophageal ganglion; longitudinal fibers to dorsal proboscis sheath (Figure 4G)
a'''.d/s	-	(0.5)+(-0)	±0.5	-	-	-	
b'''	24±1	(0.5)+(-0)	0.75±.25	22±1	51	=	No contribution. (Figure 6)
b'''.d/s	-	(0.5)+(-0)	±0.75	-	-	-	
c'''	24	(0.5)+(-0)	1±0.5	23	42	=	Circumferential fibers in the proboscis, mesenchyme and/or neurons within the presumptive anterior sucker, "fiber network" in body wall" extending to posterior sucker (Figure 5).
c'''.d/s	-	(0.5)+(-0)	≤0.5	>3	-	-	
dm'	18.5	(0.5)+(-0.25)	0.25±0.1	17.75±0.25	161	=	Bilaterally symmetric sets of epithelial cells to provisional integument, proboscis and proboscis sheath, plus putative glial cells in the sub and supraesophageal ganglia and some neurons associated with the proboscis (Figure 4H). Cell cycle composition for dnoqq' clone is identical to that of dnoqq', and is omitted.
dm'.d/s	5±0.5	(0.5)+(-0)	1±0.25	4±0.25	-	-	
dnoqq'	16±0.5	(0.5)+(-0.25)	0.25±0.12	15.25±0.25	dnoqq'	=	Epithelial cells of the provisional integument.
dnoqq'.a	8.75±0.5	(0.5)+(-0)	±0.5	7±0.5	75	=	
dnoqq'.v	10.75±0.5	(0.5)+(-0)	±0.5	10±0.5	-	=	
dnoqq'.aa	4±0.75	(0.5)+(-0)	1.25±0.25	2.5±0.5	dnoqq''	=	
dnoqq'.av	6.5±0.75	(0.5)+(-0)	1.25±0.25	5±0.5	135	=	
dnoqq'.va	4.25±0.5	(0.5)+(-0)	1±0.25	3±0.25	-	=	
dnoqq'.vv	-	(0.5)+(-0)	1.5±0.25	>3	-	=	
dnoqq'''	15±1	(0.5)+(-0)	0.5±0.25	-	328	≠	
dnoqq'''.v	6±2	(0.5)+(-0)	-	-	-	=	
dnoqq'''.a	11±2	(0.5)+(-0)	0.5±0.25	11±1.5	-	=	
dnoqq'''.va	9±2	(0.5)+(-0)	-	-	-	=	
dnoqq'''.vv	12±2	-	-	-	-	=	
dm''	18.75	(0.5)+(-0)	0.5±0.12	18	161	=	Epithelial cells to proboscis sheath (Figure 4J), connective tissue or sheath to subesophageal ganglion.
dm''.d/s	-	(0.5)+(-0)	>1	-	-	-	
nopq'	13.5	(0.5)+(-0)	0.3±0.12	12.25	220	≠	Epithelial cells to the anterior sucker and/or oral opening, plus a few neurons to the anterior portion of the subesophageal ganglion (Figure 4K). Left nopq' and nopq'' clones are bilaterally symmetric to right nopq' and nopq'' clones, respectively.
nopq'.v	5.5±0.5	(0.5)+(-0)	3±0.25	2.5±.25	-	=	
nopq'.a	-	(0.5)+(-0.25)	3.5±0.25	>8	-	=	
nopq'.va/vv	10±0.5	(0.5)+(-0)	1±0.25	8.5	-	=	
opq'	17.5±0.5	(0.5)+(-0)	0.4	17±0.5	153	=	Cells of the putative adhesive organ, anterior to the subesophageal ganglion at ventral side of the embryo (Figure 4L)
opq'.v	4.25±0.25	(0.5)+(-0)	1±0.25	2.75±0.25	-	=	
opq'.a	-	(0.5)+(-0)	1±0.25	>2.75	-	=	
opq''	9	(0.5)+(-0)	0.4	8.5	203	=	Epithelial cells to provisional integument, plus putative definitive epithelial cells to ventral and lateral surfaces of posterior sucker (Figure 4I).
opq''.d/s	-	(0.5)+(-0)	≤0.25	var	-	-	
n'	12.25±0.5	(0.5)+(-0)	0.4	11.7±0.5	132	≠	Epithelial cells to provisional integument.
n'.v/a	9±0.5	(0.5)+(-0)	≤0.25	8.5±0.5	-	=	
n'.va	-	(0.5)+(-0)	≤0.25	(var)	-	=	
n'.vv	-	(0.5)+(-0)	≤0.25	>4.5 (var)	-	=	
n'.aa'av	-	(0.5)+(-0)	≤0.25	4.5 (var)	-	=	

Cells are designated as described in the text (and see Fig. 2). Estimations of cell cycle composition were made using data from video time-lapse microscopy of labeled clones in living embryos, or from BrdUTP incorporation by groups of synchronized embryos fixed at selected time points, or both (see Materials and Methods for details).

*The total duration of the cell cycle was defined as the interval between the times at which cells rounded up in the course of successive divisions. Mitosis was not scored in these embryos, but lasts ~30 minutes in all early blastomeres examined in *H. triserialis* (Bissen and Weisblat, 1989). Time intervals are given in hours.

[†]We assume that cytokinesis initiates during mitosis and completes soon after mitosis. Thus, when a given cell at one time point was unlabeled and at the next time point (30 minutes later) it had divided and entered S phase, it meant that mitosis and G1 phase (if any) had ended within the previous 30 minutes, and that G1 phase was brief or nonexistent, denoted in this table by -0. Time points in which some portion of the newly divided cells had not yet entered S phase were interpreted as evidence of a definitive G1, but less than 0.25 hours.

[‡]The duration of S phase was estimated by the number of intervals at which BrdU was incorporated (15 pulses at 30 minute intervals).

[§]G2 phase is estimated as the time interval between the end of S phase and the point at which the cell rounds up to divide. This probably overestimates G2 duration, because mitosis usually begins before cell rounding, but the error introduced is small relative to the long G2 phases observed.

[¶]Total number of embryos used in BrdUTP pulse experiments to analyze cell cycle compositions.

**Relative sizes of sister cells (see Materials and Methods for definition of unequal division).

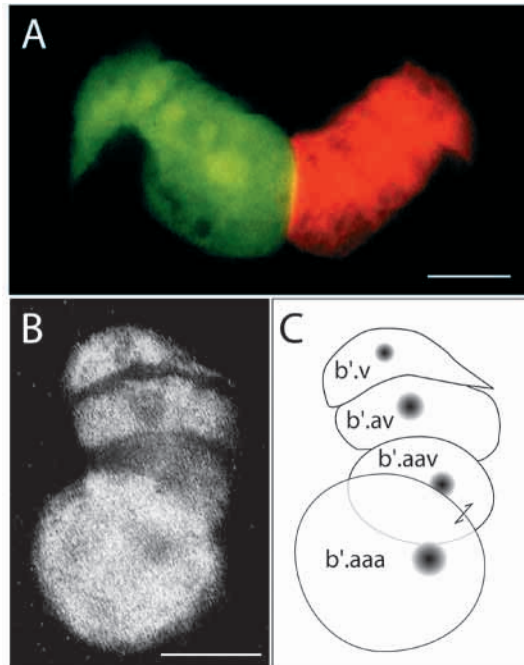


Fig. 3. Teloblastic cell divisions in the primary quartet lineages. (A) Fluorescence micrograph of an embryo at ~32 hours AZD, in which micromeres c' and d' had been injected with RDA and FDA, respectively, at ~8 hours AZD. The first few divisions of each primary quartet clone are unequal and oriented primarily along the animal-vegetal axis. The larger daughter cell lies animal to the smaller cell and has a much shorter cell cycle. Thus, a chain of cells is produced from each primary quartet micromere. (B) A higher magnification view of a slightly younger embryo in which b' had been injected with diI. (C) Disposition and identity of the cells shown in B. Double arrow indicates the progeny of the most recent cell division. Scale bars: 20 μ m.

from the subesophageal ganglion, lateral to the ventral midline within the germinal plate, reaching at least as far as midbody segment M17 (Fig. 5A-C,E). A third set of cells arising from c''' appears as mesenchyme or neurons, or both, within the presumptive anterior sucker (Fig. 5C,D).

Micromeres b'' and b''' were unique in that we were unable to detect any definitive progeny from these two cells in stage 10 embryos. In these experiments, b'' or b''' was injected in more than 70 embryos. Of these, ~40 b'' -injected and ~40 b''' -injected embryos survived to stage 10, but no labeled cells were observed in any of these specimens. Further experiments revealed that the clones arising from cells b'' and b''' die in normal development, which explains this result.

Cell fate plasticity in the b'' lineage

Previous fate mapping experiments revealed that all six 'trio micromeres' form similarly compact and well-labeled clones at clonal ages 49.7-52.2 hours (Smith and Weisblat, 1994). Using video microscopy to follow b'' and b''' clones during later development (Fig. 6), we found that small fluorescent particles appeared around the clones at some time between 50-75 hours clonal age (Fig. 6B; 60-85 hours AZD). We interpret these particles as cellular debris resulting from the death of the labeled cells. Over time, this debris either remained confined

within a fluorescent 'bag' (Fig. 6C-E) or scattered over the embryo beneath the provisional integument.

These observations confirm that the clones derived from micromeres b'' and b''' normally die prior to stage 10. Is the death of the b micromere clones induced by cell interactions? To address this question, we attempted to rescue b'' or b''' micromeres by ablating one or more nearby cells, as shown in Table 2.

Rescue of b'' was obtained in all 21 embryos in which micromere c'' was ablated. In these embryos, the distribution of the surviving b'' progeny at stage 10 resembled the normal pattern of c'' progeny (compare Fig. 4D,E; Fig. 7A,B). No rescue of b'' was obtained by ablating any other cell of those tested, including cell a'' , which makes a clone that is bilaterally symmetric to the normal c'' clone (Table 2).

As a further step towards understanding the nature of the interactions signaling the fate of the b'' clone, we performed a series of experiments in which c'' was labeled with FDA and b'' was labeled with RDA; the c'' clone was photolesioned at progressively later times and the fate of the b'' clone was determined. These experiments revealed that the b'' clone could be rescued to the normal c'' fate with 100% efficiency when it was less than 50 hours clonal age (59 hours AZD) and not at all by the time it had reached 58 hours clonal age (67 hours AZD; Fig. 8). This result suggests that the b'' is committed to die at ~50 hours clonal age, which is also the time we see the first evidence of dying cells in the b'' clone in normal development. These results do not conclusively identify the source of the fate-determining signals, and we cannot exclude the possibility of direct or indirect signaling by the debris of the lesioned c'' clone. But the simplest interpretation of our results is that the b'' clone dies in response to a signal from the c'' clone and that b'' commits to die soon after receiving the signal from the c'' clone. At this time, the b'' and c'' clones each comprise six to ten cells.

In the rescue experiments described above, the entire set of cells in the normal c'' clone arose from either c'' (in eight normal embryos; Fig. 7A) or from b'' (in 21 embryos where c'' was killed before the b'' clone committed to die; Fig. 7B) or were missing (in five embryos where the c'' clone was killed after the b'' clone was committed to die; not shown). However, in one embryo in which the c'' clone was photolesioned at 48 hours clonal age, the resultant stage 10 embryo contained an intermingled mosaic of RDA- and FDA-labeled cells (Fig. 7C); the total number of labeled cells seemed normal. We interpret this result as reflecting a partial kill of the c'' clone, with a correlated partial rescue of the b'' clone.

In contrast to the results with the b'' lineage, attempts to rescue the b''' clone were seemingly successful in only 1 of 54 experimental embryos (Table 2). In this embryo, the a''' micromere was supposed to have been ablated just prior to injecting b''' with lineage tracer, and the labeled clone closely resembled the normal a''' pattern (not shown). Given this low success rate and the technical difficulty of the experiment, it seems likely that this apparent rescue of the b''' cell resulted from accidentally killing b''' and labeling a''' with lineage tracer.

DM-derived micromeres (dm' and dm'')

Cells dm' and dm'' are similar in the duration (~19 hours) and composition of their cell cycles (Fig. 2; Table 1). Further

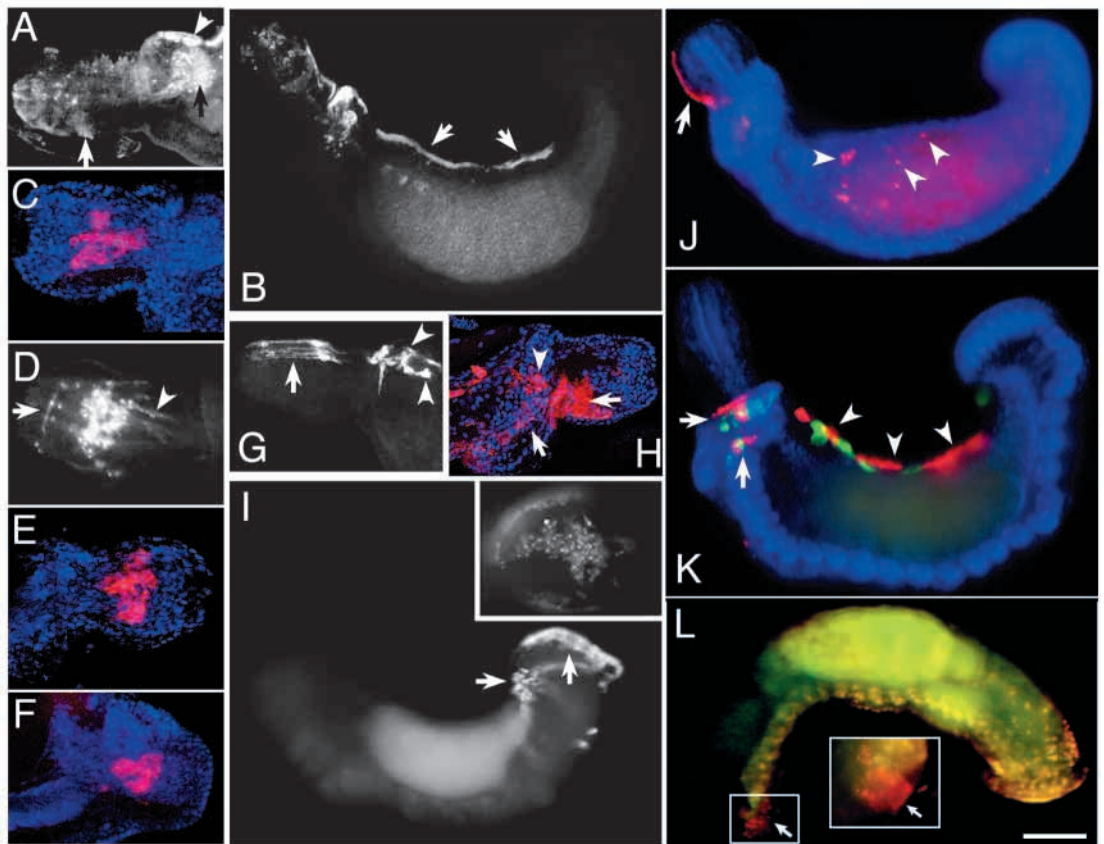
divisions have been observed only for dm' . The secondary cells divide equally and, as in other micromere lineages, with a much shorter cell cycle than the parent micromere (~5 hours).

The definitive fates of these two cells differ greatly. At stage 10, dm' gives rise to a prominent pattern of circular muscle fibers in the proboscis that is complementary to those generated by micromere c''' (Fig. 5A-C, D). In addition, as with micromere c''' , well-labeled dm' clones include one or more cells exhibiting a previously uncharacterized neuronal

morphology within the proboscis and germinal plate; thin processes of these cells seem to have grown throughout the surface of the germinal plate (Fig. 5A,B). A more prominent process runs near the lateral edge of the germinal plate for the entire length of the embryo and then ramifies just dorsal to the fused ganglia in the posterior sucker (Fig. 5E,F). A third set of cells arising from dm' appears as mesenchyme or neurons, or both, within the presumptive anterior sucker (Fig. 5C,D).

The dm' clone contributes bilaterally to the ventral covering

Fig. 4. Definitive micromere progeny; lateral views at stage 10 (160-170 hours AZD). Stacked confocal images (A-H) or epifluorescence views showing embryos in which various micromeres had been labeled with lineage tracer as indicated (anterior to left except in E,F,H,J). Most embryos were counterstained with Sytox Green (for confocal microscopy) or Hoechst 33258. (A) Anterior end of an embryo in which micromere d' was injected with RDA shows labeled progeny in supraesophageal ganglion (black arrow), prostomial epidermis (white arrow), and epithelial cells of the provisional integument (arrowhead). (B) An entire embryo in which micromere a' had been injected with RDA. This view illustrates that, in addition to the anterior cells (as in A), the primary quartet micromeres contribute



progeny to the epithelium of the provisional integument, which by stage 10 lie compressed along the dorsal midline (arrows). (C,D) Anterior ends of embryos at early and late stage 10, respectively, in which micromere a'' had been injected with RDA. At early stage 10, the a'' clone comprises an undifferentiated set of cells within the left half of the proboscis (C); by late stage 10 (D), these cells project narrow processes, suggesting that they are neurons (arrow) or connective tissue (arrowhead), or both. (E) Right side of the anterior end of an embryo in which micromere c'' had been injected with RDA (compare with C). (F) Right side of the anterior end of an embryo in which micromere b'' had been injected with RDA and micromere c'' was ablated by over-injection (compare with E). (G) Anterior end of an embryo in which micromere a''' had been injected with RDA. Progeny include putative neural or connective tissue cells (arrowheads), or both, associated with the supraesophageal ganglion and a parallel array of elongated cells (arrow), perhaps retractor muscles, within the dorsal proboscis sheath. (H) Right side of the anterior end of an embryo in which micromere $dnpq''$ had been injected with RDA. Progeny include epidermal cells of the proboscis sheath, what appear to be glial cells in the subesophageal (slanted arrow) and supraesophageal (arrowhead) ganglia, and some neurons or connective tissue in the proboscis (horizontal arrow). Micromere $dnpq''$ generates a mirror image clone on the left side of the embryo (not shown). (I) Side view, focusing on the posterior sucker, of an embryo in which micromere opq'' had been injected with RDA. Progeny include epidermal cells in the provisional integument (horizontal arrow), which are in the process of being sloughed off in this late stage 10 embryo and in the skin of the posterior sucker (vertical arrow). Inset shows a ventral view of the posterior sucker, where the opq'' -derived epidermal cells seem to persist. (J) Right side of the anterior end of an embryo in which micromere dm'' had been injected with RDA. Progeny include what appear to be epidermal cells on the outer surface of the proboscis sheath (arrow); from this clone, cell debris (arrowheads) is usually seen between the yolk cell and the germinal plate. (K) Side view of an embryo in which $nopq''_L$ had been injected with RDA and $nopq''_L$ had been injected with FDA. Both clones gives rise to epidermal cells of the provisional integument (arrowheads) plus a few neurons in the anterior portion of the subesophageal ganglion (vertical arrow) and, more anteriorly, epidermal cells in the anterior sucker or mouth, or both (horizontal arrow). Within this latter group, the $nopq'$ -derived cells invariably lie anterior to the $nopq''$ -derived cells. The right $nopq'$ and $nopq''$ clones (not shown) are bilaterally symmetric to those of the left $nopq'$ and $nopq''$ clones, respectively. (L) Side view of an embryo in which the opq' clone was uniquely labeled with RDA by injecting blastomere OPQ with RDA and OPQ' with FDA (see Materials and Methods). Progeny (arrow) comprise cells in the putative anteroventral adhesive organ. Inset shows boxed area at higher magnification. Scale bar: 50 μ m in A,C,D,H; 100 μ m in B,I-L; 50 μ m in inset to I; 30 μ m in inset to L.

of the proboscis sheath (Fig. 4J). Other dm'' progeny appear to be connective tissue or sheath associated with the anterior portion of the nerve cord, including the subesophageal ganglion. In addition, when micromere dm'' had been labeled,

we observed a random pattern of irregular fluorescent spots throughout the embryo (Fig. 4J). We interpret this material as cell debris, suggesting that a significant amount of cell death occurs among the dm'' progeny.

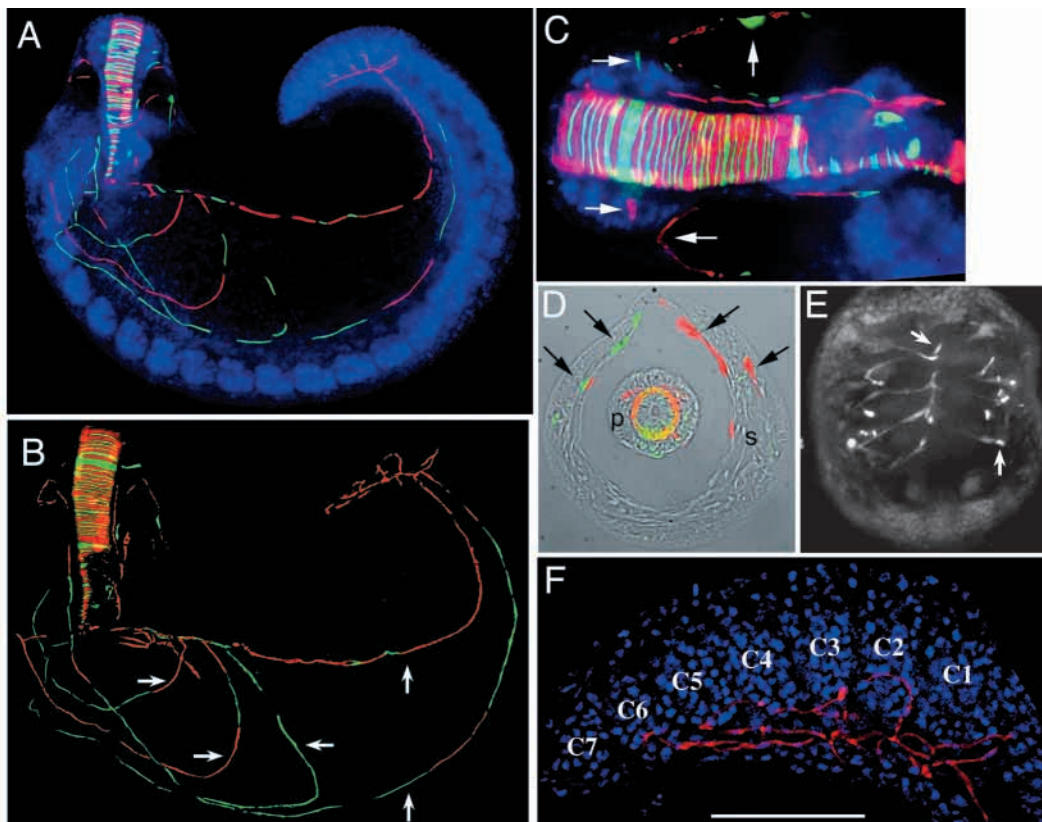


Fig. 5. Definitive progeny of micromeres dm' and c''' at stage 10 (~160 hours AZD). (A) Digital montage, combining the in focus portions of 59 optical sections (10 \times , 0.45 NA objective; 0.8 μ m steps; 2D 'no neighbors' deconvolution (Metamorph, UIC) of each section prior to montaging) comprising a side view through an embryo in which micromere dm' had been injected with RDA and micromere c''' with FDA (dorsal is up; anterior to the left; see Materials and Methods for details). (B) The same embryo and imaging procedures as in A, but viewed through a 20 \times , 0.75 NA objective for higher resolution (74 optical sections; 0.7 μ m steps), and without the Hoechst fluorescence images, to bring out the details of the labeled cells. The dm' and c''' clones contribute prominent, interdigitated sets of circumferential fibers, presumably muscles, to the proboscis. Additional labeled cells lie within the proboscis (arrows in C), some of which appear to be part of a most curious and hitherto undescribed network of nonsegmental, interconnected fibers that reaches throughout the body wall of the embryo. (The following abbreviated description of this network was drawn from observations of more than 15 embryos in which both c''' and dm' were labeled, three in which c''' alone was labeled and six in which dm' alone was labeled.) The network consists of five main fibers on each side of the animal. Two roughly parallel fibers on each side (vertical arrows) run the length of the animal near the surface of the body wall; a dorsolateral fiber runs near the edge of the germinal plate and a ventromedial fiber lies $\sim 1/4$ of the distance from the ventral midline to the dorsal midline. These two fibers extend to the posterior end, where one or both ramify just dorsal to the seven fused ganglia that innervate the tail sucker. Within the anterior midbody, three more main fibers on each side loop between the dorsolateral and ventromedial fibers, at the approximate levels of midbody segments 2, 5 and 8 (horizontal arrows). Additional fibers are present in the anterior midbody segments, but could not be reconstructed in their entirety. This accounts for apparent discontinuities in some fibers; note that many breaks in the fibers in the low resolution image (A) are shown to be continuous in the higher resolution image (B). Note in particular that individual, apparently continuous fibers comprise juxtaposed segments of distinct red (dm' -derived) and green (c''' -derived) cells. (C) Lateral view of the proboscis of the same preparation (anterior towards the left, dorsal is upwards) using the same imaging procedures as in A,B, but viewed through a 40 \times , NA 0.75 objective (29 optical sections; 0.5 μ m steps). Arrows indicate additional cells within the proboscis and proboscis sheath. (D) Combined fluorescence and brightfield (DIC optics) images of a transverse plastic section ($\sim 10 \mu$ m) through the proboscis at about the level of the vertical arrow in C. Circumferential fibers are visible within the proboscis (p). Segments of the fiber network (arrows) are visible in the sheath (s). (E) Digital montage of fluorescence micrographs made from three obliquely horizontal plastic sections ($\sim 10 \mu$ m each) through the dorsal region of the posterior sucker in a roughly horizontal plane (anterior is upwards). The dm' -derived region of the fiber network ramifies in a bilaterally symmetric fashion (better visible on the left, owing to the oblique plane of section). The branches tend to lie between the seven segmental ganglia that have fused to form the caudal ganglion (see also A). Some cell bodies are visible (arrows). (F) Digital montage of the developing posterior sucker of the embryo shown in A,B (20 \times , 0.75 NA objective; 58 sections, 0.7 μ m steps) showing a side view of the ramifying fibers in the tail sucker, just dorsal to the seven fused ganglia (C1-C7). To maintain the same orientation as in A,B, prospective dorsal is downwards in this panel, owing to the curvature of the embryo. Scale bar: 100 μ m in A,B; 50 μ m in C-F.

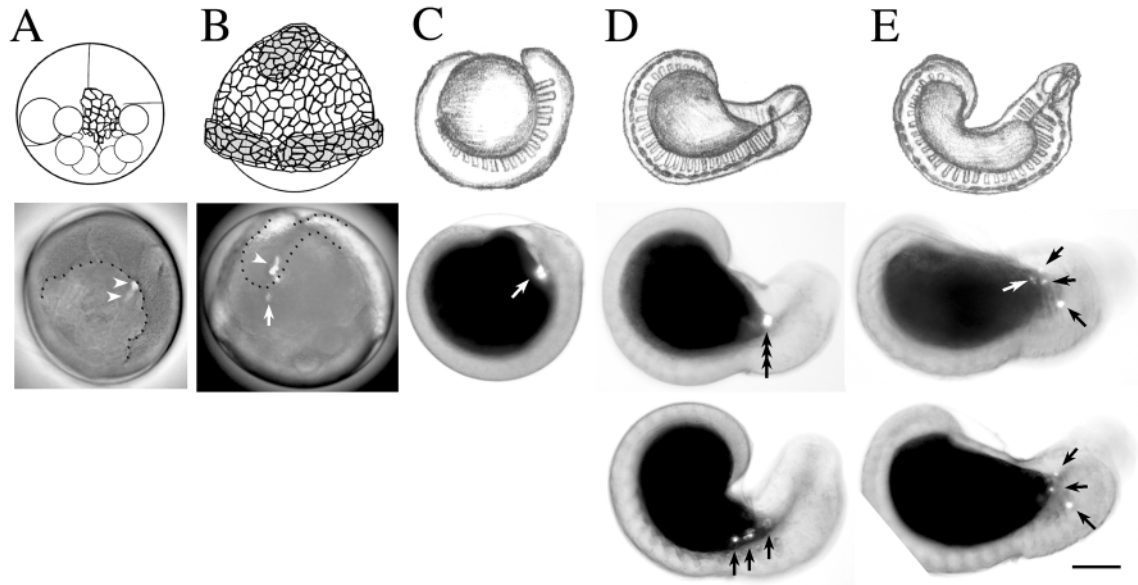


Fig. 6. Rise and fall of the micromere b''' clone in normal development. Combined brightfield and fluorescence live images of one typical embryo (22 total) in which micromere b'' had been injected with RDA (0 hours clonal age, 12 hours AZD, not shown). (A) Animal view at 24 hours clonal age (36 hours AZD; see Fig. 1); the labeled clone comprises two cells (arrowheads) within the micromere cap (dotted contour). (B) Dorsal view at 63 hours clonal age (75 hours AZD, see Fig. 1). By this point, the clone (arrowhead) comprises six to ten cells within the anterior portion of the germinal plate (dotted contour shows germinal plate and part of right germ band), but cell death is probably already under way, as evidenced by isolated cellular debris (arrow). (C) Lateral view at 111 hours clonal age (123 hours AZD); by this stage the remnants of the b''' clone (arrow) are confined to a fluorescent 'bag' trapped between the germinal plate and the yolk. (D,E) Each panel shows two closely timed (~ 0.5 second apart) lateral views at 129 hours (D) or 147 hours (E) clonal age (141 and 159 hours AZD, respectively). Once the embryo has initiated peristalsis, the fluorescent remnants of the b''' clone (arrows) can be seen to drift back and forth in response to muscle contractions. The b'' clone follows a very similar time course (not shown). Scale bar: 100 μm .

DNOPQ-derived micromeres ($dnopq'$, $dnopq''$ and $dnopq'''$)

As outlined by Dohle (Dohle, 1999), the particular pattern of divisions by which the ectodermal precursor cell DNOPQ (micromere 2d in classic nomenclature) makes three micromeres before dividing equally to form left and right homologs is a characteristic and highly conserved feature of annelid development. Our results extend previous observations (Smith and Weisblat, 1994) that cells $dnopq'$ and $dnopq''$ act as left/right homologs, whereas $dnopq'''$ follows a different fate.

Table 2. Ablation of neighboring micromeres can rescue the b'' clone, but not b'''

	Scored	Ablated	<i>n</i>	Fate
	b''	c'' and b'''	9	b'' replaces c''
		b'''	15	death
		c''	12	b'' replaces c''
		a''	13	death
	b'''	a''' and b''	9	death
		a'''	45	death

In each of 103 embryos, either b'' or b''' was injected with RDA; one or more neighboring micromeres was ablated by over-injection and the fate of the RDA-labeled clone was determined. The diagram on the right depicts the relative positions of the various micromeres after a''' and b''' are born, but experiments involving b'' were initiated before those cells arise.

Similarities between $dnopq'$ and $dnopq''$, and the differences between these cells and $dnopq'''$, are apparent as soon the cells are born, in that $dnopq'$ and $dnopq''$ exhibit a 15 minute G1 phase that is absent in $dnopq'''$. The brief G1 phase in these cells was not observed by previous workers (Bissen and Weisblat, 1989), presumably because the 30 minute pulses of BrdUTP incorporation they employed did not permit them to discriminate shorter events. By contrast, we find no G1 phase for $dnopq'''$ even using 15 minute pulses of BrdUTP. We described two to three further cell cycles in each of the three $dnopq$ micromere lineages (Table 1, Fig. 2). Divisions in the $dnopq'$ lineage preceded those in the $dnopq''$ lineage by the amount expected from the 1 hour difference in the times of their births. As for the other lineages, the secondary cells generally divided more rapidly than did the parent micromeres. Cell $dnopq'''$ divides unequally after ~ 15 hours, giving a smaller cell ($dnopq'''a$) closer to the primary quartet micromeres and a larger cell ($dnopq'''v$) closer to the OPQ blastomeres. The daughters of micromere $dnopq'''$ exhibited much greater variability in cell cycle duration than for any lineage, except opq'' and n' , ranging from 4 to 8 hours for $dnopq'''p$ and from 9 to 13 hours for $dnopq'''a$.

As previously described for stage 7 (Smith and Weisblat, 1994), $dnopq'$ and $dnopq''$ clones appeared as a left/right pair at stage 10. Each clone contributes cells to the epithelium of the provisional integument (not shown), to the epithelium of the proboscis and its sheath, plus what appear to be glial cells in the subesophageal and supraesophageal ganglia and some neurons associated with the proboscis (Fig. 4H). Later still, cell

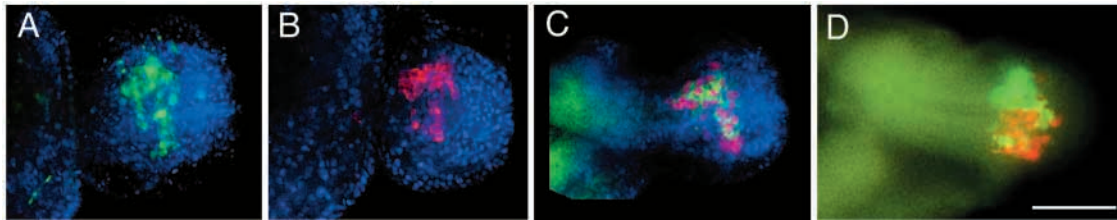


Fig. 7. Micromere fate differences between *H. robusta* (Sacramento) and *Helobdella* sp. (Galt). Fluorescence micrographs of stage 10 embryos in which micromeres b'' and c'' had been injected with RDA and FDA, respectively. (A–C) *H. robusta* (Sacramento). (A) In normal development, c'' contributes a group of cells to the proboscis (see also Fig. 4), and the b'' clone has died. (B) When c'' is ablated (by photolesioning at clonal age 36 hours; see Fig. 8), the b'' clone survives and generates a set of cells resembling the normal c'' progeny. (C) In a single embryo in which the c'' clone was photolesioned at clonal age 48 hours, some progeny of both b'' and c'' survived and intermingled both anteroposteriorly and dorsoventrally. (D) In contrast to the foregoing, the normal development of *Helobdella* sp. (Galt) entails the contribution of definitive progeny by both micromeres b'' and c'' . Note that in this species, the b'' and c'' progeny are largely confined to the ventral and dorsal portions of the proboscis, respectively. Scale bar: 50 μ m.

debris is observed just within the anterior ventral body wall when either $dnopq'$ or $dnopq''$ are labeled (not shown), suggesting that significant numbers of cells die in both these clones.

Micromere $dnopq'''$ gives rise exclusively to epithelial cells of the provisional integument (Smith and Weisblat, 1994). By stage 10, all the remaining cells in this clone lay along the dorsal midline (not shown).

NOPQ-derived micromeres ($nopq'_{L/R}$ and $nopq''_{L/R}$)

Although the left and right $nopq'$ and $nopq''$ micromeres arise as true bilateral homologs, we have observed slight but reproducible differences in the cell cycles of the parent NOPQ blastomeres. Thus, the right $nopq'$ and $nopq''$ micromeres are each born \sim 5 minutes before their contralateral homologs. In contrast to most other serially produced micromeres but similar to $dnopq'$ and $dnopq''$, micromeres $nopq'$ and $nopq''$ seem to follow quite similar fates, as judged both by their division patterns and by the fates of their clones at stage 10.

Immediately upon their birth, cells $nopq'$ and $nopq''$ go into a 20 minute S phase followed by a 12.5 hour G2 phase. Each of these micromeres divides unequally, giving rise to a smaller animal cell ($nopq'.a$; $nopq''.a$) and a larger vegetal cell ($nopq'.p$; $nopq''.p$) having roughly twice the diameter. Both sister cells exhibit an S phase of \sim 3 hours duration, but although the larger cell in each pair has a 2.5 hour G2 phase, the small cell in each pair has a G2 phase longer than 8 hours. The larger cells ($nopq'.v$ and $nopq''.v$) divide after 5.5 hours and give rise to equal-size daughter cells with no detectable G1 phase and an S phase of \sim 1 hour duration.

By stage 10, each $nopq'$ and $nopq''$ clone has contributed some epithelial cells to the provisional integument; epidermal cells to the anterior sucker or oral opening, or both; plus a few neurons to the anterior portion of the subesophageal ganglion. As expected, the left $nopq'$ and $nopq''$ clones are bilaterally symmetric to those of the right $nopq'$ and $nopq''$ clones, respectively. On each side, the contributions of $nopq'$ and $nopq''$ are similar, but not identical (Fig. 4K). Moreover, ablating the $nopq'$ cells does not affect the fates of the $nopq''$ cells, and vice versa (data not shown).

OPQ-derived micromeres ($opq'_{L/R}$ and $opq''_{L/R}$)

Of all the 25 micromeres, the pair of opq' cells are the most

difficult to observe or label by direct microinjection (Smith and Weisblat, 1994). The cells are born beneath the micromere cap between cells N and OPQ'; attempts to inject them with lineage tracer often result in labeling other micromeres. For this reason, we used a subtractive method (Smith and Weisblat, 1994; Zackson, 1982) for labeling opq' clones, injecting OPQ with RDA and OPQ' with FDA, so that the opq' clone was uniquely labeled with RDA only. By contrast, the opq'' micromeres arise in a prominent location between the OPQ' blastomeres and are easily identified and injected.

The opq' cells have a cell cycle of \sim 17.5 hours, most of which is spent in G2 phase. There is no detectable G1 phase and S phase lasts only \sim 25 minutes. The division is somewhat unequal, yielding a larger cell called $opq'.v$ (proximal to the teloblasts) and a smaller cell called $opq'.a$ (distal to the teloblasts). Cell $opq'.v$ divides \sim 4 hours later (Table 1); we did not observe the division of $opq'.a$ in the time periods we sampled, up to 22 hours clonal age of the parent opq' micromere.

At stage 10, the opq' clone is confined to a structure located

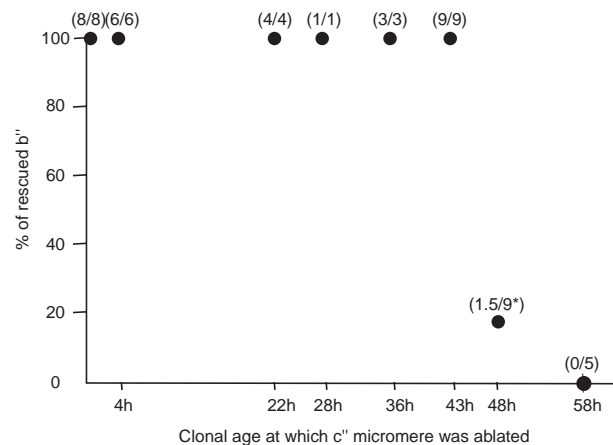


Fig. 8. Time dependence of b'' rescue. Except for the earliest time point (at which micromere c'' was killed directly by over-injection), the c'' clone was photolesioned at selected intervals after injecting c'' with FDA and b'' with RDA (see Materials and Methods for details). The star indicates one of the nine embryos tested at clonal age 48 hours that exhibited in a partial rescue (see Fig. 7C).

anterior to the subesophageal ganglion at or near the surface on the ventral side of the embryo (Fig. 4L). We believe that this structure is the adhesive organ by which the embryos normally attach to the ventral surface of their parent in the time interval between hatching from the cocoon and developing a functional rear sucker.

The first division of opq'' is equal and occurs 9 hours after its birth, yielding cells $opq''.d$ and $opq''.s$. For these daughter cells, S phase is as rapid as in a teloblast, lasting less than 15 minutes, but the overall cell cycle is much longer, ranging from 11 to 14 hours for both cells. There is no fixed order to the divisions of $opq''.d$ and $opq''.s$ and the subsequent divisions of cells in the opq'' clone are rapid but variable in terms of orientation and timing. The average size of the opq'' clone increases from 4.5 ± 0.8 ($n=6$) cells at 21.75 hours clonal age to 6.8 ± 1.1 ($n=6$) cells at 24.25 hours clonal age. The indeterminacy of the divisions in the opq'' clones (along with the n' and $dnopq'''$ clones) correlates with the fact that they give rise to a pure and apparently homogeneous population of epithelial cells for the provisional integument. By stage 10, the opq'' clones occupy the posterior end of the dorsal midline and on the ventral and lateral surfaces of the posterior sucker (Fig. 4I).

N-derived micromeres ($n'_{L/R}$)

The first division of n' is unequal and occurs ~12 hours after birth. S phase in the progeny lasts less than 15 minutes and the larger, more vegetal, cell $n'.v$ divides first, after ~9 hours. As in the $dnopq'''$ and opq'' clones, subsequent divisions in the n' clones are equal and variable in terms of timing and orientation. G1 phase is lacking and S phase seems constant and usually short (15 minutes or less) in these cells; thus, the variability is due to variable length of G2 phase.

Micromere n' gives rise exclusively to epithelial cells of the provisional integument (Smith and Weisblat, 1994). By stage 10 (155 hours AZD), no remnant of the n' clone could be detected.

Micromere fate differences between *H. robusta* (Sacramento) and *Helobdella* sp. (Galt)

In the course of our experiments, we had occasion to use embryos from leeches collected from a site near Galt, California, roughly ten miles from where the paratype and holotype *H. robusta* were obtained (Shankland et al., 1992). We initially assumed that these leeches were simply another population of *H. robusta*, and as expected, their embryonic development was indistinguishable from that of the Sacramento population in most respects (data not shown). Two sets of observations put this assumption of identity in doubt, however, and comparisons of mitochondrial DNA sequences strongly suggest that they are in fact two different species (F. Z. Huang and A. E. Bely, personal communication).

First, in embryos of *Helobdella* sp. (Galt), the clone of micromere b'' did not die. Instead (Fig. 7D), b'' and c'' each contributed to a set of neurons similar to those arising exclusively from c'' in *H. robusta* (Sacramento). The contributions from b'' and c'' did not intermingle, in contrast to the one *H. robusta* (Sacramento) in which both b'' and c'' clones survived (Fig. 7C). Second, in *Helobdella* sp. (Galt), micromere c''' does die, and circumferential fibers in the proboscis arise entirely from micromere dm' (not shown).

These differences between *Helobdella* sp. (Galt) and *H. robusta* (Sacramento) were observed with complete reproducibility (25 embryos from two different individuals for *Helobdella* sp. (Galt) and more than 70 embryos from more than seven individuals for *H. robusta* (Sacramento)).

DISCUSSION

Micromere lineages in leech

In glossiphoniid leeches, 25 small cells arise during cleavage (7-22 hours AZD in *H. robusta*). This set of cells is not identical to cells defined as micromeres according to the classical notions of spiral cleavage, but we group them together as micromeres in *Helobdella* because they all contribute to nonsegmental tissues, and exclude others ($2d=DNOPQ$ and $4d=DM''$) because they are proteloblasts. It had been shown previously that, by the onset of epiboly (~60 hours AZD), these micromeres in *Helobdella* embryos make stereotyped contributions of cells either to the superficial epithelium of the provisional integument, or to sets of deep cells that presumably contributed to definitive nonsegmental tissues of the adult leech, or both (Smith and Weisblat, 1994). These contributions are stereotyped in terms of the approximate size and location of the clones and the distribution of their cells between deep and superficial layers.

We have further characterized the micromere lineages in two ways. First, we have detailed the initial division in each micromere lineage in terms of cell cycle duration and composition, and the symmetry and orientation of the divisions. Second, we have mapped their descendant clones to 160 hours AZD, by which time the adult body plan is clear and terminal differentiation of most cell types is well underway. The main conclusions of this work given below.

With certain exceptions, the lineages of individual micromeres appear to be as stereotyped as those of the segmental founder cells: no G1 phase was observed in primary micromeres; S and G2 phases varied considerably in different lineages; some micromeres divide equally and others undergo unequal divisions.

Although most of the micromere lineages are idiosyncratic, we find that $nopq'$ and $nopq''$ have identical early patterns of cleavages and cell cycle composition and also give rise to intermingled sets of epithelial progeny at early epiboly (Smith and Weisblat, 1994). Despite these similarities, the ipsilateral $nopq'$ and $nopq''$ clones are not equivalent. Smith and Weisblat (Smith and Weisblat, 1994) showed that killing $nopq''$ does not alter the distribution of the $nopq'$ progeny in early epiboly, and we have extended this result to the definitive progeny in stage 10.

Exceptions to the stereotypy of the micromeres lineages were found in micromeres that give rise to exclusively epithelial progeny (i.e. $dnopq'''$, $opq''_{L/R}$ and $n'_{L/R}$). These five lineages show much greater variability in cell cycle duration, beginning either with the primary micromere (in the case of $dnopq'''$) or with its immediate progeny (in the case of $opq''_{L/R}$ and $n'_{L/R}$). In all five of these lineages, the variability is first evident in the duration of G2 phase, and not S phase. Variability in cell cycle duration occurs from cell to cell within these clones, rather than on a clone to clone basis, so that the order of cell divisions within these five clones also varies.

As described previously (Smith and Weisblat, 1994), we found that opq'' clones proliferate at about twice the rate of the $dnopq'''$ clones. Our present results indicate that this difference in proliferation rate results simply from differences in the average cell cycle duration between the clones and not from a difference in the pattern of cell division (i.e. not a case of geometric versus arithmetic proliferation).

For most of the cells studied, there is no obvious pattern to the cell divisions, but the primary quartet micromeres (a' , b' , c' and d') are an exception. For at least the first three cell divisions, all four of these cells exhibit teloblastic, stem-cell-like divisions. These divisions are unequal in terms of cell size; the larger sister cell lies posterior to the smaller one in each case and also has a shorter cell cycle time (Fig. 2; Fig. 3). The divisions are also unequal in cell fate, in that the smaller cells contribute exclusively to the superficial epithelium, whereas the larger, posterior cell is the one that ultimately contributes 'deep', definitive progeny to the supraesophageal ganglion and other nonsegmental tissues, as well as additional superficial epithelial cells. The point at which the deep and superficial cell fates are finally segregated remains to be determined.

As reported previously (Smith and Weisblat, 1994), micromeres b'' and b''' contribute exclusively deep progeny at the onset of epiboly. And like the other cells that contribute exclusively to 'deep cells' (a'' , a''' , c'' , c''' , dm' , dm'' , $opq'_{L/R}$), b'' and b''' undergo a long G2 phase (~22 hours) prior to an equal first division. Thus, the discovery that neither micromere b'' nor b''' make any definitive contribution to the embryo was unexpected. Moreover, the observation that these cells can be killed at birth without observable effects on development suggests that their clones are vestigial in *H. robusta*.

The finding that micromere b'' can be rescued and induced to follow the c'' fate when micromere c'' is killed suggests that micromeres b'' and c'' constitute an equivalence group, in which giving rise to the normal c'' clone is the primary fate, and in which the secondary fate is cell death. By contrast, we found no combination of ablations that was able to rescue the b''' clone.

Comparison with other leeches and oligochaetes

The patterns of micromere-forming divisions in *H. robusta* (Smith and Weisblat, 1994) are essentially identical to those in two other glossiphoniid leech species that have been examined, namely *Theromyzon tessulatum* (Sandig and Dohle, 1988) and *Helobdella triserialis* (Bissen and Weisblat, 1989). This is not surprising given the extensive conservation of micromere-forming cleavage patterns throughout the Annelida (Dohle, 1999).

The only other annelid for which a comparable analysis of embryonic cell cycle compositions has been carried out is the closely related species *H. triserialis*, by Bissen and Weisblat (Bissen and Weisblat, 1989), who did not treat all the micromeres or any of their progeny. The cell cycles for which data is available from both species exhibit similar compositions, except that S phase in the secondary and tertiary micromere trios ranges from 55 to 90 minutes in *H. robusta* (Table 1), significantly longer than the 15 minute S phases of the their homologs in *H. triserialis* (Bissen and Weisblat, 1989).

Given this extensive conservation of cleavage patterns and micromere cell cycle compositions, we were particularly

surprised to find clear, qualitative differences in the fates of certain micromeres between two leeches that we initially assumed were the same species. In each population (*H. robusta* (Sacramento) and *Helobdella* sp. (Galt)), one micromere dies that makes definitive progeny in the other population. One can imagine that such cells are now 'evolutionarily available' for the production of novel structures.

Comparison with mollusks: cellular origins of bilateral symmetry

The Spiralia comprise about ten phyla, among which Annelida and Mollusca are the most speciose. Current molecular phylogenies suggest that all spiralian fall within the clade Lophotrochozoa, and that the spiral cleavage pattern reflects a well-conserved ancestral condition, in contrast to the wide variety of adult body plans. It has been proposed that equal cleavage (i.e. specification of the D quadrant by inductive interactions) and indirect development via a trochophore larva were basal traits in both annelids and mollusks (Freeman and Lundelius, 1992), but the former conclusion has been questioned for annelids (Dohle, 1999). In any event, comparisons of micromere fates and fate specification mechanisms between annelids and mollusks should provide insights into the ancestral condition of these taxa and the processes by which they diverged.

Molluscan cell cycle compositions have been most carefully described for *Lymnaea stagnalis*, an equal cleaver (van den Biggelaar, 1971a; van den Biggelaar, 1971b). In *Lymnaea*, the first three cell cycles are of equal length and composition; at the 24-cell stage, there is a pause in cell division that correlates with the shift of macromere 3D towards the center of the embryo. This pause entails a more than twofold prolongation of the cell cycles for the 24 blastomeres present (macromeres 3A-3D, micromeres 3a-3d and the eight daughters of the first two micromere quartets). The main conclusion of this work was that the changes in cell cycle duration in *Lymnaea* were achieved mainly by lengthening G2 phase; no G1 phase was detected in any of these cells.

Comparing *Helobdella* and *Lymnaea*, there are dramatic differences in the absolute and relative lengths of analogous cell cycles. Overall, early cell cycles are much slower in *Helobdella* than in *Lymnaea* (3-24 hours at 23°C versus 1.3-6.7 hours at 25°C, respectively), and we detect no global pause in early cell divisions in *Helobdella*. Moreover, in *Helobdella* the cell cycles of the secondary trio micromeres are prolonged like those of the tertiary trio, whereas in *Lymnaea*, the analogous cells (quartet 2a-2d) divide with a relatively rapid time course like the primary quartet micromeres. In *Helobdella*, as in *Lymnaea*, changes in cell cycle duration in the early embryo are achieved mainly by changes in the length of G2 phase (Bissen and Weisblat, 1989), although we did detect significant cell-specific differences in the duration of S phase, and brief G1 phases in the secondary trio of micromeres.

Regarding micromere cell fates, two carefully characterized mollusks are the gastropods *Patella vulgata*, an equal cleaver (Damen and Dictus, 1994) and *Ilyanassa obsoleta*, an unequal cleaver (Render, 1991; Render, 1997). Both *Patella* and *Ilyanassa* are highly derived relative to the ancestral mollusk, which presumably resembled the bilaterally symmetric Monoplacophorans. Among annelids, there is no clear candidate for the most basally derived group, but the leeches,

as direct developing clitellates, are also highly derived. Although it is therefore impossible to make detailed comparisons between micromere fates in annelids and mollusks at present, our results reveal significant differences between leeches and mollusks, even in terms of how bilateral symmetry is generated from these spiral cleaving embryos.

Bilateral symmetry becomes evident at various points in the modified spiral cleavages of *Helobdella*, *Ilyanassa* and *Patella*. The formation of bilateral mesendoderm (in mollusk) and segmental mesoderm (in leech) from the equal division of micromere 4d (DM'' in leech) is regarded as an ancestral spiralian trait (Brusca and Brusca, 1990). Similarly, micromere 2d in *Patella* makes a bilaterally symmetric contribution to post-trochal ectoderm and apparently establishes left and right precursors at its first division (Damen and Dictus, 1994); the homologous cell in leech, proteloblast DNOPQ, serves as a precursor of segmental ectoderm for both sides of the leech, but only after making three micromeres (dnopq'-dnopq'''), which seem to be lacking in *Patella*. The dnopq' and dnopq'' micromeres give rise to bilaterally symmetric clones, despite the fact that they arise by sequential divisions (of DNOPQ and DNOPQ'). As expected, the bilateral pairs of micromeres arising from the further cleavages in the NOPQ lineages (i.e. nopq'_L and nopq'_R, and nopq''_L and nopq''_R also form bilaterally symmetric clones; this paper) (Smith and Weisblat, 1994).

Another way in which leech differs from the typical pattern of spiral cleavage is that the micromeres arising from the B quadrant arise with opposite handedness to those in the other three quadrants (Sandig and Dohle, 1988; Bissen and Weisblat, 1989) and thus mirror symmetric orientation with respect to the A quadrant micromeres. This correlates with clear differences between leech and mollusk in terms of micromere fates, and is summarized below.

In *Patella*, micromeres 1a and 1c contribute progeny to the left and right sides, respectively, as do cells 2a and 2c contribute mirror symmetric clones to the left and right sides; the clones of cells 1b, 1d, 2b and 2d, however, each more or less straddle the midline (Dictus and Damen, 1997). The same holds true for *Ilyanassa* (except that in the primary quartet, it is the combined 1a and 1d clones that comprise the mirror image of the 1c clone) (Render, 1991), which suggests that the plane of bilateral symmetry bisects the B and D quadrants. In *Helobdella*, by contrast, primary quartet micromeres a' and b' appear as left/right homologs (as do c' and d') in terms of their early lineages (this paper), the morphogenetic movements of their clones (Nardelli-Haeffliger and Shankland, 1993) and the definitive fates of their progeny (this paper). Within the secondary trio, we have shown that b'' normally makes no definitive contribution and that a'' and c'' normally give rise to bilaterally symmetric clones, as in the mollusks. But we also find that when c'' is ablated, b'' assumes the c'' fate and thus is capable of serving as a contralateral homolog to a''.

In the third quartet of micromeres, symmetry relationships differ. In *Patella* and *Ilyanassa*, cells 3a and 3b form clones that are mirror images of one another, as do cells 3c and 3d (Dictus and Damen, 1997; Render, 1997), whereas in *H. robusta*, the clones of the three micromeres that contribute definitive progeny all straddle the midline. Among these, c''' and dm' (homologs of 3c and 3d, respectively) give rise to seemingly identical clones. As in the second tier of

micromeres, the third B quadrant micromere also fails to contribute definitive progeny, but within this group, b''' is not capable of replacing a''' or c'''. Whether this constellation of differences between the micromere cell fates in annelid and mollusk will hold true for more basally derived representatives of the two phyla remains to be determined. In any event, we propose that the situation in leech represents an evolutionary 'transition' in which the A and B lineages are becoming true contralateral homologs.

This work was supported by NSF grants IBN 9723114 and 0091261 and NASA grant FDNAG2-1359 to D. A. W. and by NSF grant IBN 9817384 to S. T. B.

REFERENCES

- Aguinaldo, A. M. A., Turbeville, J. M., Linford, L. S., Rivera, M. C., Garey, J. R., Raff, R. A. and Lake, J. A. (1997). Evidence for a clade of nematodes, arthropods and other moulting animals. *Nature* **387**, 489-493.
- Anderson, D. T. (1973). Embryology and phylogeny in annelids and arthropods. Oxford, New York: Pergamon Press.
- Bissen, S. T. and Weisblat, D. A. (1989). The durations and compositions of cell cycles in embryos of the leech, *Helobdella triserialis*. *Development* **106**, 105-118.
- Brusca, R. C. and Brusca, G. J. (1990). *Invertebrates*. Sunderland, MA: Sinauer.
- Damen, P. and Dictus, W. J. A. G. (1994). Cell lineage of the prototroch of *Patella vulgata* (Gastropoda, Mollusca). *Dev. Biol.* **162**, 364-383.
- Dictus, W. J. A. G. and Damen, P. (1997). Cell-lineage and clonal-contribution map of the trochophore larva of *Patella vulgata* (Mollusca). *Mech. Dev.* **62**, 213-226.
- Dohle, W. (1999). The ancestral cleavage pattern of the clitellates and its phylogenetic deviations. *Hydrobiologia* **402**, 267-283.
- Fernández, J. (1980). Embryonic development of the glossiphoniid leech *Theromyzon rude*: characterization of developmental stages. *Dev. Biol.* **76**, 245-262.
- Fernandez, J. and Olea, N. (1982). Embryonic development of glossiphoniid leeches. In *Developmental Biology of Freshwater Invertebrates* (ed. F. W. Harrison and R. R. Cowden), pp. 317-361. New York: Alan R. Liss.
- Fischer, A. (1999). Reproductive and developmental phenomena in annelids: a source of exemplary research problems. *Hydrobiologia* **402**, 1-20.
- Freeman, G. and Lundelius, J. W. (1992). Evolutionary implications of the mode of D quadrant specification in coelomates with spiral cleavage. *J. Evol. Biol.* **5**, 205-247.
- Ho, R. K. and Weisblat, D. A. (1987). A provisional epithelium in leech embryo: cellular origins and influence on a developmental equivalence group. *Dev. Biol.* **120**, 520-534.
- Huang, F. Z. and Weisblat, D. A. (1996). Cell fate determination in an annelid equivalence group. *Development* **122**, 1839-1847.
- Nardelli-Haeffliger, D. and Shankland, M. (1992). Lox2 a putative leech segment identity gene is expressed in the same segmental domain in different stem cell lineages. *Development* **116**, 697-710.
- Nardelli-Haeffliger, D. and Shankland, M. (1993). Lox10, a member of the NK-2 homeobox gene class, is expressed in a segmental pattern in the endoderm and in the cephalic nervous system of the leech *Helobdella*. *Development* **118**, 877-892.
- Render, J. (1991). Fate maps of the first quartet micromeres in the gastropod *Ilyanassa obsoleta*. *Development* **113**, 495-502.
- Render, J. (1997). Cell fate maps in the *Ilyanassa obsoleta* embryo beyond the third division. *Dev. Biol.* **189**, 301-310.
- Sambrook, J., Maniatis, T. and Fritsch, E. F. (1989). *Molecular Cloning: A Laboratory Manual*. Cold Spring Harbor, N.Y.: Cold Spring Harbor Laboratory Press.
- Sandig, M. and Dohle, W. (1988). The cleavage pattern in the leech *Theromyzon tessulatum* (Hirudinea, Glossiphoniidae). *J. Morphol.* **196**, 217-252.
- Shankland, M., Bissen, S. T. and Weisblat, D. A. (1992). Description of the Californian leech *Helobdella robusta*, new species, and comparison with *Helobdella triserialis* on the basis of morphology, embryology, and experimental breeding. *Can. J. Zool.* **70**, 1258-1263.

- Smith, C. M. and Weisblat, D. A.** (1994). Micromere fate maps in leech embryos: lineage-specific differences in rates of cell proliferation. *Development* **120**, 3427-3438.
- Symes, K. and Weisblat, D. A.** (1992). An investigation of the specification of unequal cleavages in leech embryos. *Dev. Biol.* **150**, 203-218.
- van den Biggelaar, J. A. M.** (1971a). Timing of the phases of the cell cycle during the period of asynchronous division up to the 49-cell stage in *Lymnaea*. *J. Embryol. Exp. Morph.* **26**, 367-391.
- van den Biggelaar, J. A. M.** (1971b). Timing of the phases of the cell cycle with tritiated thymidine and Feulgen cytophotometry during the period of synchronous division in *Lymnaea*. *J. Embryol. Exp. Morph.* **26**, 351-366.
- Wedeen, C. J., Price, D. J. and Weisblat, D. A.** (1990). Analysis of the life cycle, genome, and homeo box genes of the leech *Helobdella triserialis*. In *The Cellular and Molecular Biology of Pattern Formation* (ed. D. L. Stocum and T. L. Karr), pp. 145-167. New York: Oxford University Press.
- Weisblat, D. A., Kim, S. Y. and Stent, G. S.** (1984). Embryonic origins of cells in the leech *Helobdella triserialis*. *Dev. Biol.* **104**, 65-85.
- Zackson, S. L.** (1982). Cell clones and segmentation in leech development. *Cell* **31**, 761-770.